# Superior anti-poisoning performance of graphenes versus carbon nanotubes as Pt catalysts supports for formate oxidation

**ARTICLE** *in* INTERNATIONAL JOURNAL OF HYDROGEN ENERGY · DECEMBER 2015

Impact Factor: 3.31 · DOI: 10.1016/j.ijhydene.2015.11.033

INTERNATIONAL JOURNAL OF HYDROGEN ENERGY XXX (2015) 1–8

Available online at www.sciencedirect.com

ScienceDirect

journal homepage: www.elsevier.com/locate/he

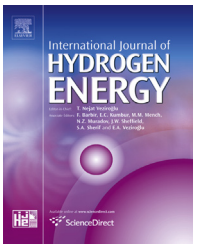

# Superior anti-poisoning performance of graphenes versus carbon nanotubes as Pt catalysts supports for formate oxidation

*Jianshe Wang* [a,b,*], *Changhai Liu* [b,c], *Mohammad Norouzi Banis* [b], *Niancai Cheng* [b], *Adam Riese* [b], *Suidong Wang* [c], *Xueliang Sun* [b,c,*]

[a] *School of Chemical Engineering and Energy, Zhengzhou University, Zhengzhou 450000, PR China*
[b] *Department of Mechanical and Materials Engineering, The University of Western Ontario, ON, N6A 5B9, Canada*
[c] *Soochow University-Western University Joint Centre for Synchrotron Radiation Research, Institute of Functional Nano & Soft Materials (FUNSOM), Soochow University, Suzhou, Jiangsu 215123, PR China*

ARTICLE INFO

*Article history:*
Received 22 July 2015
Received in revised form
4 November 2015
Accepted 5 November 2015
Available online xxx

*Keywords:*
Formate oxidation
Pt
Anti-poisoning performance
Graphene
Carbon nanotubes
Characterization

ABSTRACT

Pt nanoparticles were prepared and deposited on carbon nanotubes (CNTs) and graphene nano-sheets (GNs) to obtain composites of Pt/CNTs and Pt/GNs, respectively. The morphologies of Pt particles for the two catalysts were observed using transmission electron microscopy (TEM). It showed that the average Pt sizes for Pt/CNTs and Pt/GNs are similar, meaning that the differences in the electrochemical performance of the two catalysts could be ascribed to support effects. Pt/CNTs and Pt/GNs were quantitatively compared by simultaneously analyzing their cyclic voltammetry (CV) and chronoamperometry (CA) data for formate oxidation, showing that Pt/GNs is evidently superior to Pt/CNTs in terms of anti-poisoning performance. CO stripping on the two catalysts indicated that the strength of CO adsorption on GNs-supported Pt is weaker than that for CNTs-supported Pt. The X-ray photoelectron spectroscopy (XPS) spectra showed that the binding energy of Pt 4f for Pt/GNs was higher than that for Pt/CNTs, indicating a stronger interaction of Pt with GNs than with CNTs and consequently a weaker adsorption of CO on GNs-supported Pt. We believe that this study can be used as a guide for future evaluation and screening of supports and/or anode catalysts for direct liquid fuel cells.



## Introduction

Direct liquid fuel cells (DLFCs) such as direct formic acid fuel cells [1–3] and direct alcohols fuel cells [4–6] have gained intensive research interest in the last two decades because of their promising potential as power sources for automobiles and portable electronics. However, there are still several issues to be solved before the commercialization of DLFCs. For example, the fuels crossover needs to be mitigated and the oxygen reduction kinetics needs to be enhanced [7–11]. As for the anode catalysts, which usually are Pt- and Pd-based, one

* *Corresponding authors*. Department of Mechanical and Materials Engineering, The University of Western Ontario, ON, N6A 5B9, Canada. Tel.: +1 519 661 2111x87759; fax: +1519 661 3020.
E-mail addresses: wangjs07@zzu.edu.cn (J. Wang), xsun@eng.uwo.ca (X. Sun).

http://dx.doi.org/10.1016/j.ijhydene.2015.11.033



Please cite this article in press as: Wang J, et al., Superior anti-poisoning performance of graphenes versus carbon nanotubes as Pt catalysts supports for formate oxidation, International Journal of Hydrogen Energy (2015), http://dx.doi.org/10.1016/j.ijhydene.2015.11.033

urgent task is to simultaneously improve the activity and anti-poisoning performance. As is well-known, these performances can be enhanced usually through engineering the composition or structure of metallic catalysts [12–14]. The use of suitable supports is another way to improve catalysts performances. Carbon nanotubes (CNTs) and graphene nanosheets (GNs), featuring facile availability, high electronic conductivity and large surface area, have been reported as typical Pt and Pd supports materials to exhibit excellent performance [15–17]. However, accurate comparisons between CNTs and GNs in terms of anti-poisoning performance are still seldom reported.

When evaluating the effect of carbonaceous supports on activity of DLFCs anode catalysts, one universal method is cyclic voltammetry (CV) technique. It is noteworthy herein that CV method has also been widely adopted to judge the anti-poisoning performance of DLFCs anode catalysts by calculating the ratio of peak current during the forward scan ($I_f$) to that during the backward scan ($I_b$) [18–25]. The major premise for this application is that $I_b$ is caused by the oxidation of residual carbon species and a higher ratio of $I_f/I_b$ means better anti-poisoning performance [18]. However, Hofstead-Duffy et al. have pointed out that this premise is not sufficiently justified and the current ratio criterion is an inadequate parameter to assess the anti-poisoning performance of an anode catalyst [26]. On the other hand, although a high activity for a catalyst could be obtained from its CV data, the current obtained from chronoamperometry (CA) test, in some case, was inappropriately low, mainly resulting from the severe deactivation caused by poisoning species [6,27,28]. Therefore, the CA results are more closely related with the true anti-poisoning performance of a catalyst than CV results. However, to our knowledge, most comparisons of CA results for two catalysts are presented as qualitative analysis neither considering the difference in initial voltammetric currents nor caring the details of CA current decay [22–24], making the obtained conclusion less informative. Therefore, it is necessary to establish a quantitative and rational method for fully assessing the anti-poisoning performance based upon CA and CV results.

In the past a few years, direct formate fuel cells (DFFCs) have gained increasing interest partly because of the low overpotential of formate oxidation and favorable oxygen reduction kinetics in alkaline media [29–36]. To date, limited studies on anode catalysts for DFFCs have been focused upon the metallic Pt or Pd moieties [29–32] with no attention paid to various supports such as CNTs or GNs. As has been demonstrated, formate oxidation on Pt suffers distinct poisoning [31,32]. This can make the difference in anti-poisoning effects of carbonaceous supports more sensitively evidenced, and at the same time, demonstrate urgent demand for selecting superior supports with excellent anti-poisoning performance. Bearing this in mind, in this study, we prepared Pt catalysts supported on CNTs and GNs, and then quantitatively compared the CA data based upon the initial CV currents of formate oxidation on the two catalysts. We found that GNs can exert more distinct anti-poisoning effect on Pt when compared with CNTs, exemplifying an efficient avenue for catalyst improvement through support optimization. We believe that the characterization method employed in this study can be accepted as a general prototype for evaluating and screening of supports and/or anode catalysts for DLFCs other than DFFCs.

## Experimental

### Chemicals

Multi-walled carbon nanotubes (CNTs) were obtained from Shenzhen Nanotech Port Co., Ltd. and the average diameter of CNTs are 40–60 nm $H_2PtCl_6 \cdot 6H_2O$, potassium formate (HCOOK) and other reagents were of analytical purity and used without further purification.

Graphite oxide was obtained following a modified Hummers methods previously reported by our group [37]. The graphite oxide was then rapidly exfoliated to obtain graphene via a thermal treatment at 1050 °C under Ar atmosphere.

### Preparation of Pt catalysts supported on CNTs and GNs

CNTs (300 mg) were first treated by boiling the as-received CNTs in $HNO_3$ (69 wt. %, 30 mL) for 3 h [38] to introduce oxygen-containing group for subsequent Pt deposition. Pt precursor was reduced by ethylene glycol (EG) under microwave heating [39]. Briefly, 60 mL EG solution in a beaker containing 240 mg NaOH and 106 mg $H_2PtCl_6 \cdot 6H_2O$ was heated to boil through 1 min microwave radiation. The obtained Pt nanoparticles in EG solution were equally divided into two parts and added drop-wise into a beaker containing 50 mg CNTs or GNs dispersed by magnetic stirring. After 3 h adsorption of Pt onto CNTs or GNs, 1 mL of each mixture was centrifuged and the supernatant liquid for Pt and CNTs mixture showed light yellow color while the supernatant liquid for Pt and GNs mixture was colorless, indicating that some Pt particles have not been adsorbed on CNTs. To promote Pt deposition on CNTs or GNs, aqueous HCl solution was dropwise added to the two mixtures until the pH was below 2. Then each mixture was stirred for further 10 min, filtered, washed with de-ionized water, and dried in a vacuum oven at 70 °C. The sample was denoted as Pt/CNTs or Pt/GNs, the Pt content in which was determined using inductively coupled plasma (ICP) emission spectrometer to be 20 wt. % and 26 wt. %, respectively.

### Physical characterization of Pt/CNTs and Pt/GNs

The X-ray diffraction (XRD) patterns of Pt/CNTs and Pt/GNs were recorded on a Bruker D8 Advance X-ray diffractometer using Cu-K$\alpha$ as the radiation source.

The morphology of Pt particles was examined with transmission electron microscopy (TEM, FEI Quanta FRG 200F, operating at 200 kV). The corresponding size distribution histograms were obtained by measuring more than 200 Pt particles for each sample.

The electronic structures of the Pt particles were characterized with the X-ray photoelectron spectroscopy (XPS, Kratos Axis Yltra DLD, monochromatic Al K$\alpha$) in ultrahigh vacuum.

Please cite this article in press as: Wang J, et al., Superior anti-poisoning performance of graphenes versus carbon nanotubes as Pt catalysts supports for formate oxidation, International Journal of Hydrogen Energy (2015), http://dx.doi.org/10.1016/j.ijhydene.2015.11.033

### *Electrochemical characterization of Pt/CNTs and Pt/GNs*

Catalysts inks were first prepared for coating on a glassy carbon (GC, $\Phi = 5$ mm) electrode. Specifically, 2 mg Pt/CNTs or Pt/GNs was mixed with 600 uL ethanol containing 0.4 mg Nafion® (4.4 mg Nafion® was used for preparing Pt/GNs ink) and ultrasonicated for 30 min to form homogeneous PtCNTs ink, then 15 μL ink was pipetted onto the GC electrode and dried using an infrared lamp.

A three-electrode cell coupled with an Autolab potentiostat/galvanostat (Model PGSTAT-30, Ecochemie, Brinkman Instrument) was used for electrochemical characterization. A GC electrode, a Pt wire electrode and a Hg/HgO electrode were used as working electrode, counter electrode and reference electrode, respectively. All potentials herein were referred to Hg/HgO electrode, and all the electrochemical experiments were conducted at 25 °C in a $N_2$-saturated solution.

For each catalyst characterization, CV was first conducted at 50 mV $s^{-1}$ in 1 M KOH solution until stable cyclic voltammograms (CVs) were recorded. Then CVs for formate oxidation were recorded in 1 M KOH + 1 M HCOOK solution by starting from −0.8 V, followed by corresponding CA tests conducted at −0.5 V for 2500 s. It is noteworthy herein that all the working electrode was preconditioned at 0.3 V for 3 s before recording the CVs or CA data for formate oxidation.

For CO stripping experiments, gaseous CO was bubbled into the electrolyte (1 M KOH) for 30 min to allow adsorption of CO onto the electro-catalysts while maintaining a constant voltage of −0.8 V. Excess CO in solution was purged out with $N_2$ for 20 min. Then two successive CVs for CO stripping were recorded at a scan rate of 20 mV $s^{-1}$.

## Results and discussion

### *XRD and HRTEM results for Pt/CNTs and Pt/GNs*

The XRD patterns of Pt/CNTs and Pt/GNs are shown in Fig. 1. The peak at 26.4° in the XRD patterns of Pt/CNTs and Pt/GNs can be ascribed to the carbon (002) plane diffraction. The four peaks including Pt(111) at 39.8°, Pt(200) at 46.1°, Pt(220) at 67.8° and Pt(331) at 81.6° confirmed the presence of metallic Pt in both samples [40]. The main peak at 39.0° in the XRD pattern of Pt/GNs is somewhat broadened in comparison with the Pt(111) for Pt/CNTs, indicating the average grain size of Pt in Pt/GNs is smaller than that in Pt/CNTs. This is possibly because of the aggregation of Pt particles or failed adsorption of certain smaller Pt particles during preparation of Pt/CNTs, as analyzed according to the following high resolution TEM (HRTEM) results.

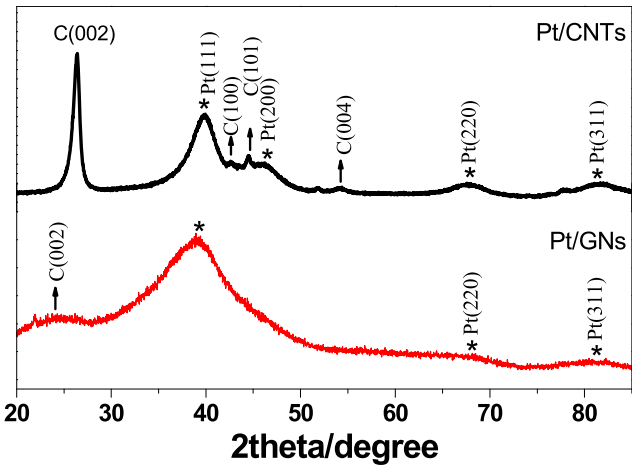


**Fig. 1 – The XRD patterns of Pt/CNTs and Pt/GNs.**

The HRTEM images of Pt/GNs and Pt/CNTs are shown in Fig. 2(a) and (b) and the corresponding Pt size distribution histograms are presented in Fig. 2(c) and (d). As seen in Fig. 2(a), the platinum particles are uniformly dispersed on GNs. The inset micrograph shows the lattice distance of Pt particles (~0.230 nm) ascribed to (111) lattice planes, indicating the crystallinity of face-centered cubic (fcc) structure. The mean Pt size for Pt/GNs was measured to be ~1.5 nm by averaging over 200 particles, as shown in Fig. 2(b). For the HRTEM of Pt/CNTs, however, most Pt particles are linked together forming one dimensional nanostructures and some apparent aggregations of Pt particles can be seen. The mean Pt sizes for Pt/CNTs are ~2.1 nm, a little larger than that of Pt/GNs. To analyze the possible reason for this result, it is worth explaining that the properties of Pt in Pt/CNTs and Pt/GNs were designed to be completely identical by first preparing Pt particles in a single beaker and then depositing these Pt particles on CNTs and GNs supports, respectively. During preparation of Pt/GNs, we found that the Pt particles can be easily deposited on GNs (judging from the colorless supernatant liquid after centrifugation), possibly because of the larger surface area and more defects on GNs. However, for Pt/CNTs, it was seen that not all Pt particles were deposited on CNTs even after adding HCl to promote Pt deposition. It is possible that the lost Pt particles might be smaller-sized since particles smaller than 1 nm cannot be found in Pt/CNTs, as indicated from Fig. 2(d), resulting in an increased average Pt size. There is also another possibility that some Pt particles smaller than 1 nm were combined with larger ones into aggregates when using HCl to promote Pt deposition. We also noticed that the lattice lines of certain amount of Pt particles in close connection are in consistent alignment, as shown in the inset of Fig. 2(c). This alignment and the Pt aggregation would produce distinctly narrower Pt diffraction peak for the XRD patterns of Pt/CNTs in comparison with Pt/GNs.

### *Electrochemical characterization of Pt/CNTs and Pt/GNs*

For electrochemical characterization of Pt/CNTs and Pt/GNs, CV tests were first conducted within a potential range from −0.8 V to 0.2 V until stable CVs were obtained. By doing so, the possible evolution of Pt surface structure caused by high potential limit can be alleviated. After recording stable CVs in 1 M KOH and 1 M KOH + 1 M HCOOK solution, three cycles of CVs ranging from −0.8 V to 0.3 V were then recorded at 50 mV $s^{-1}$ and 10 mV $s^{-1}$, respectively. The cyclic voltammetric profiles of the second and third cycles overlap well, so only the CVs for the first (red dashed lines) and second cycles (blue dash dot lines) were shown in Fig. 3. The CVs of Pt/CNTs and Pt/GNs in 1 M KOH solution were also recorded at 50 mV $s^{-1}$ for reference (black lines).

Please cite this article in press as: Wang J, et al., Superior anti-poisoning performance of graphenes versus carbon nanotubes as Pt catalysts supports for formate oxidation, International Journal of Hydrogen Energy (2015), http://dx.doi.org/10.1016/j.ijhydene.2015.11.033

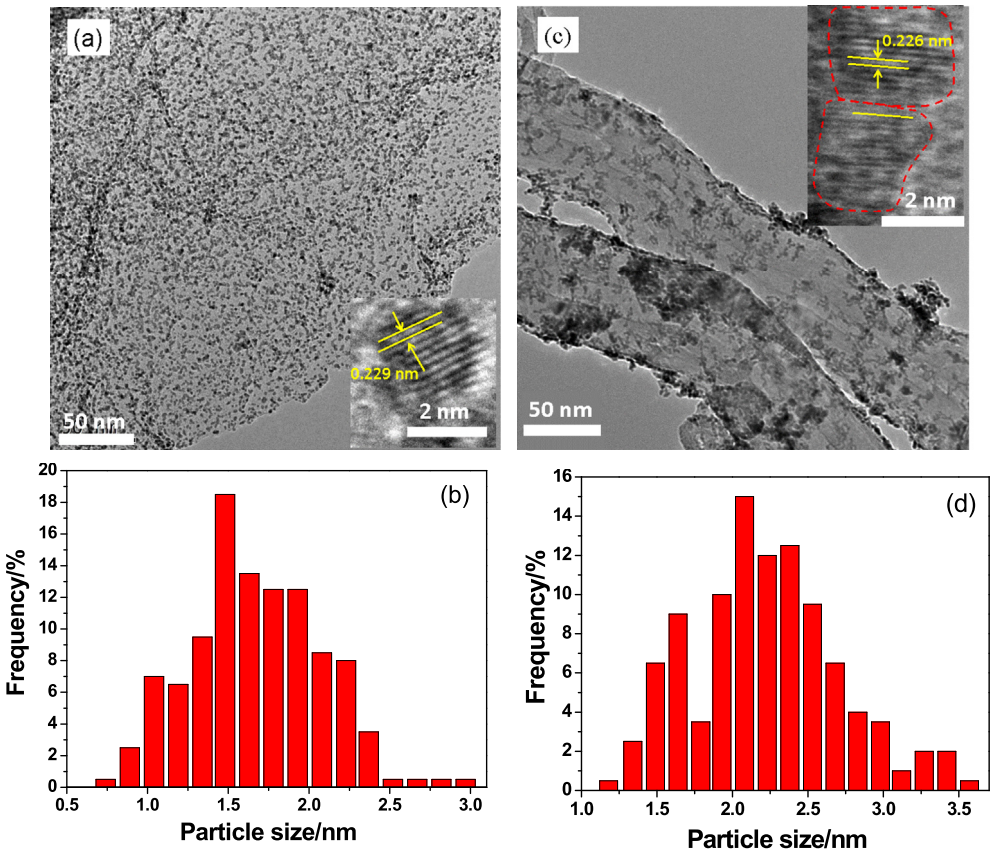


**Fig. 2 – (a) HRTEM image and (b) size distribution histogram for Pt/GNs. (c) HRTEM image and (d) size distribution histogram for Pt/CNTs.**

From Fig. 3 we can see that the first and the second cycles differ greatly in the CV profiles of Pt/CNTs and Pt/GNs. Specifically, the currents of peak 1 decrease while those of peak 2 increase for the second cycle of CVs in comparison with the first cycle. In fact, Jiang et al. [31] and John et al. [32] have thoroughly investigated formate oxidation on Pt catalysts. They ascribed the first peak to the direct formate oxidation to $CO_2$. For the second peak, which was ascribed to the indirect oxidation path, the poisoning species ($CO_{ad}$) on Pt surface were oxidized at a higher potential. According to their investigation, these poisoning species can form on Pt surface in a potential range as low as that of the H-sorption region, as evidenced from Fig. 3(a) and (b). Taking Fig. 3(a) for instance, we can see that the H adsorption and desorption profiles in the H-sorption region (−0.8 V ~ −0.4 V) are clearly seen for Pt/CNTs in 1 M KOH solution. For Pt/CNTs in 1 M KOH + 1 M HCOOK solution, the H desorption feature diminishes possibly because of the adsorption of formate ion and poisoning $CO_{ad}$. It is noteworthy herein that the first cycle of CVs (red dashed line) was recorded after preconditioning the electrode at 0.3 V for 3 s. By such preconditioning, the poisoning species on Pt surface could be cleaned. For the second cycle (blue dash dot line) without such a treatment, the poisoning species on Pt surface would inhibit the hydrogen adsorption and correspondingly the hydrogen desorption feature diminished more than that of the first cycle. Moreover, these $CO_{ad}$ species also suppressed the formate oxidation current (peak 1) in the second cycle of CVs, while the corresponding current of peak 2 increased resulting from the oxidation of these accumulated poisoning species. In fact, the above observation and analysis are also true for Pt/GNs (see Fig. 3(b)), indicating the presence of poisoning species on Pt/CNTs and Pt/GNs at lower potential range.

The effect of poisoning species on Pt/CNTs and Pt/GNs can be more clearly evidenced from Fig. 3(c) and (d). Fig. 3(c) shows the first and second cycle of CVs for Pt/CNTs recorded at 10 mV $s^{-1}$ in 1 M KOH + 1 M HCOOK solution. Because the scanning rate in Fig. 3(c) is slower than in Fig. 3(a), the corresponding time is longer for poisoning species to accumulate on Pt surfaces before being oxidized, so the feature of peak 2 (ascribed to oxidation of poisoning species) in the first cycle of CVs is more distinct in contrast to that in Fig. 3(a). In the second cycle of CVs, the current of peak 1 decreased while the current of peak 2 increased simultaneously with a higher extent in comparison with the case of Fig. 3(a), also because of the longer time of accumulation of poisoning species on Pt.

Similar to the case of Pt/CNTs in Fig. 3(c), the lower scanning rate also produced similar results on Pt/GNs, as seen in Fig. 3(d). However, the effect of poisoning species on Pt/CNTs and Pt/GNs are somewhat different. For example, the decreasing extent of current of peak 1 in the first cycle of CVs in Fig. 3(d) vs. Fig. 3(b) seems smaller than that of Fig. 3(c) vs. Fig. 3(a). This difference indicates a higher anti-poisoning performance of Pt/GNs in comparison with Pt/CNTs. To gain a more accurate insight into this difference, we collected data from Fig. 3 and made relevant calculation, as shown in Table

Please cite this article in press as: Wang J, et al., Superior anti-poisoning performance of graphenes versus carbon nanotubes as Pt catalysts supports for formate oxidation, International Journal of Hydrogen Energy (2015), http://dx.doi.org/10.1016/j.ijhydene.2015.11.033

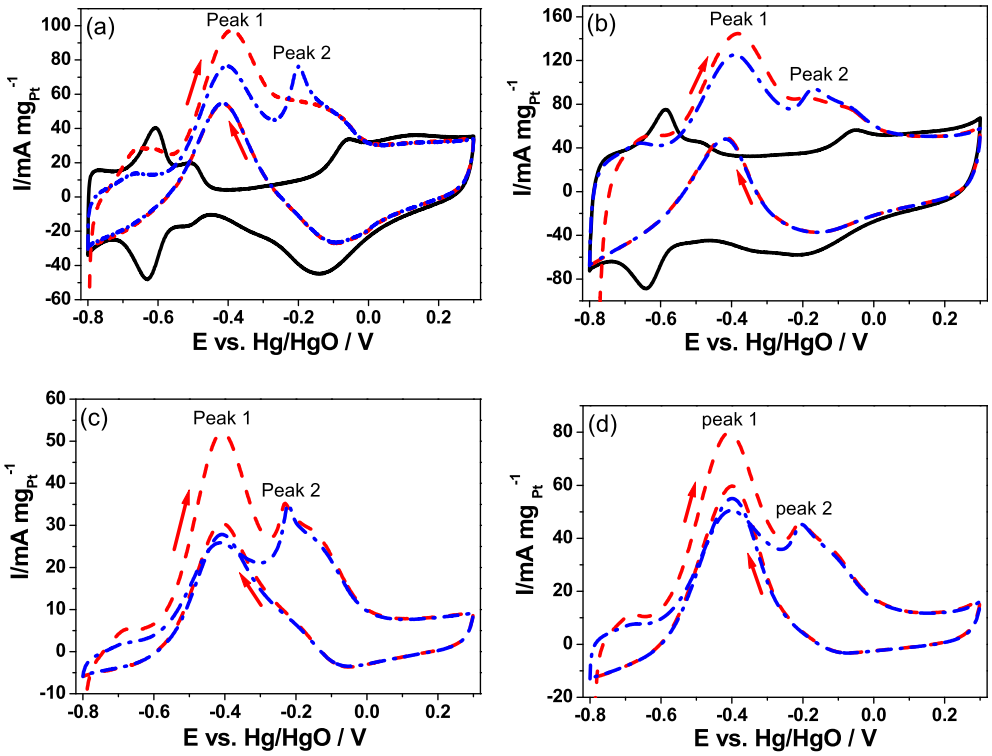


**Fig. 3 – CVs recorded in 1 M KOH + 1 M HCOOK for (a) Pt/CNTs at 50 mV $s^{-1}$, (b) Pt/GNs at 50 mV $s^{-1}$, (c) Pt/CNTs at 10 mV $s^{-1}$ and (d) Pt/GNs at 10 mV $s^{-1}$. The red dashed lines and the blue dash dot lines show the CVs of the first and second cycles. The black solid lines in (a) and (b) represent the CVs recorded in 1 M KOH at 50 mV $s^{-1}$. (For interpretation of the references to colour in this figure legend, the reader is referred to the web version of this article.)**

**Table 1 – Anti-poisoning performance of Pt/CNTs and Pt/GNs analyzed from CV results in Fig. 3.**

| Catalyst: scan rate | $I_{1-1}$/ mA $mg_{Pt}^{-1}$ | $I_{2-1}$/ mA $mg_{Pt}^{-1}$ | $I_{1-1}/I_{2-1}$ | $I_{2-2}$/ mA $mg_{Pt}^{-1}$ | $I_{2-2}/I_{2-1}$ |
|---|---|---|---|---|---|
| Pt/CNTs: 50 mV $s^{-1}$ | 72 | 63 | 1.1 | 30 | 0.48 |
| Pt/CNTs: 10 mV $s^{-1}$ | 47 | 21 | 2.2 | 13 | 0.62 |
| Pt/GNs: 50 mV $s^{-1}$ | 93 | 83 | 1.1 | 19 | 0.23 |
| Pt/GNs: 10 mV $s^{-1}$ | 69 | 43 | 1.6 | 9 | 0.21 |

1. $I_{1-1}$ and $I_{2-1}$ in Table 1 represent the currents of peak 1 recorded in the first and second cycles of CVs while $I_{2-2}$ represents the current of peak 2 in the second cycle of CVs. The ratio of $I_{1-1}$ to $I_{2-1}$ (denoted as $I_{1-1}/I_{2-1}$) means the decreasing extent of current of peak 1 caused by poisoning species formed in the second cycles, while the ratio of $I_{2-2}$ to $I_{2-1}$ (denoted as $I_{2-2}/I_{2-1}$) represents the relative strength of indirect oxidation currents (being related with the oxidation of poisoning species) with reference to direct oxidation currents. A higher value of $I_{1-1}/I_{2-1}$ or $I_{2-2}/I_{2-1}$ represents a higher tendency of poisoning.

From Table 1 we can see that the values of $I_{1-1}/I_{2-1}$ for Pt/CNTs at 50 mV $s^{-1}$ are similar as that for Pt/GNs, indicating that the difference in anti-poisoning effect of Pt/CNTs and Pt/GNs cannot be distinguished in this case. This can be explained from the aspect of negligible amount of poisoning species. Because the pretreatment at 0.3 V before recording the first cycle of CVs cleaned nearly all the poisoning species and the time is short for these species to accumulate on Pt surface at a scan rate of 50 mV $s^{-1}$, the amounts of poisoning species are therefore too low to produce discernible difference in the values of $I_{1-1}/I_{2-1}$ for Pt/CNTs and Pt/GNs. When the scanning rate is lowered to be 10 mV $s^{-1}$, the time is longer for certain amount of poisoning species to accumulate on Pt surface, and thus the difference in anti-poisoning performance of Pt/GNs and Pt/CNTs can be reflected. In this case, the value of $I_{1-1}/I_{2-1}$ for Pt/CNTs (2.2) is evidently higher than that for Pt/GNs (1.6), and the values of $I_{2-2}/I_{2-1}$ for Pt/CNTs are higher than those for Pt/GNs, indicating a superior anti-poisoning performance of Pt/GNs to Pt/CNTs.

To further verify the superior anti-poisoning performance of Pt/GNs to Pt/CNTs, CA was conducted by recording quasi-steady currents of formate oxidation on Pt/GNs and Pt/CNTs at −0.5 V. As shown in Fig. 4, both Pt/CNTs and Pt/GNs witnessed a sharp drop of current in the earlier time range and then both CA currents gradually reached quasi-steady states. During the whole time range the CA current of Pt/GNs is higher than that of Pt/CNTs. Since the initial CV currents at 0.5 V are different for Pt/CNTs and Pt/GNs (see Fig. 3), it is reasonable to use the CV currents as reference for comparing the relative current decay. In fact, Zhang et al. [41] have adopted such a method for assessment of catalysts deactivation, in which the CA currents were divided by corresponding CV currents as reference. It is noteworthy that the CV currents

Please cite this article in press as: Wang J, et al., Superior anti-poisoning performance of graphenes versus carbon nanotubes as Pt catalysts supports for formate oxidation, International Journal of Hydrogen Energy (2015), http://dx.doi.org/10.1016/j.ijhydene.2015.11.033

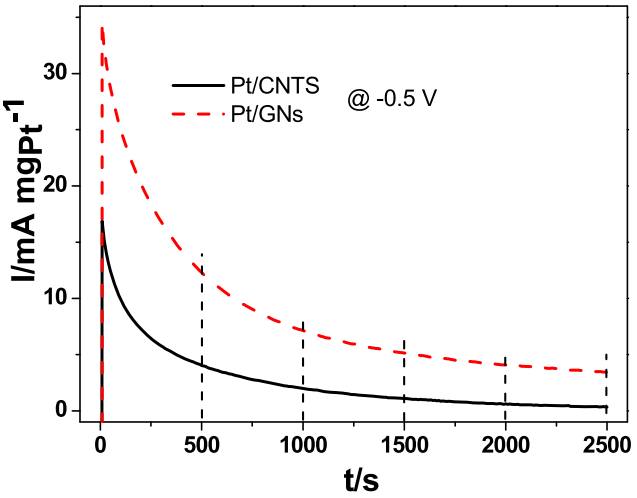


**Fig. 4 – CA curves recorded at −0.5 V in 1 M KOH + 1 M HCOOK for Pt/CNTs and Pt/GNs.**

in Zhang's work were recorded at quite a slow scanning rate (1 mV $s^{-1}$) for obtaining quasi-steady currents. However, for the present case of formate oxidation on Pt catalysts, large amounts of poisoning species would accumulate on Pt surface if the scanning rate is too low, as just analyzed in Fig. 3. Therefore, the first cycle of CVs recorded at 50 mV $s^{-1}$ were used as reference, from which the net CV currents for formate oxidation at −0.5 V were obtained to be 17.5 mA $mg_{Pt}^{-1}$ for Pt/CNTs and 31.0 mA $mg_{Pt}^{-1}$ for Pt/CNTs by subtracting the corresponding background currents.

To gain more detailed insights into the Pt deactivation based upon the CA data in Fig. 4, we propose two indices for evaluating the anti-poisoning performance, namely, relative reactivity retention (RRR) and deactivation rate (DR). The RRR is defined as $I_{CA}/I_{CV}$, where the $I_{CA}$ refers to the CA current at certain time point while the $I_{CV}$ refers to the corresponding CV current at −0.5 V obtained from the forward scanning curve. According to this definition, a higher value of $I_{CA}/I_{CV}$ for a catalyst means a higher anti-poising performance, or said another way, a lower extent of deactivation. On the other hand, the DR is defined as $\Delta I/I(t_1)$, where ΔI represents the difference between two CA currents recorded at an initial time ($t_1$) and another subsequent time ($t_2$) while $I(t_1)$ represents the CA current at $t_1$. Taking $I_{CV}$ as reference, the DR can also be represented as ΔRRR/RRR(t1), where ΔRRR represents the difference between two RRR values at $t_1$ and $t_2$ and $RRR(t_1)$ represents the RRR value at $t_1$. By calculating the DR values from the CA curves, we can measure the changes of deactivation rate during the whole time range of CA test. The RRR and DR data were calculated from Fig. 4 and listed in Table 2.

**Table 2 – Comparing the anti-poisoning performance of Pt/CNTs and Pt/GNs based upon CA and CV results.**

| | | 500 s | 1000 s | 1500 s | 2000 s | 2500 s |
|---|---|---|---|---|---|---|
| $I_{CA}$/mA $mg_{Pt}^{-1}$ | Pt/CNTs | 4.04 | 1.98 | 1.10 | 0.62 | 0.34 |
| | Pt/GNs | 12.30 | 7.15 | 5.15 | 4.07 | 3.43 |
| RRR/% | Pt/CNTs | 23.1 | 11.3 | 6.3 | 3.5 | 1.9 |
| | Pt/GNs | 39.7 | 23.1 | 16.6 | 13.1 | 11.1 |
| DR/% | Pt/CNTs | – | 51.1 | 44.2 | 44.4 | 45.7 |
| | Pt/GNs | – | 41.8 | 28.1 | 21.1 | 15.3 |

From Table 2 we can see that the RRR values of Pt/CNTs at different time points are all smaller than those of Pt/GNs. At the ending time point of CA tests, the RRR value for Pt/GNs (11.1%) is far higher than that for Pt/CNTs (1.9%), further confirming the superior anti-poisoning effect of Pt/GNS in comparison with Pt/CNTs. On the other hand, the difference in anti-poisoning performance between Pt/GNs and Pt/CNTs can also be discerned from the DR values. As seen from Fig. 4, the rates of currents decay for Pt/CNTs and Pt/GNs during the final quasi-steady time range seem similar. However, if comparing the DR values for Pt/CNTs and Pt/GNs (see Table 2), we can see that the DR values for Pt/CNTs remain relatively higher while those for Pt/GNs keep decreasing with time, indicating a higher deactivation rate of Pt/CNTs in comparison with Pt/GNs.

To gain the possible reason for the different anti-poisoning performance of Pt/GNs and Pt/CNTs, CO stripping was conducted on the two catalysts in 1 M KOH solution by assuming CO as a model poisoning species (Fig. 5). It can be seen that there are three peaks (peak 1–3) for CO stripping on Pt/CNTs and Pt/GNs. For peak 1, the CO species must be adsorbed with higher strength because the stripping potential is higher, while for peak 3 the CO species must be weakly adsorbed on certain sites. At the higher potential range (−0.3 V ~ −0.15 V), the peak 1 on Pt/CNTs lies in a slightly lower potential than the case of Pt/GNs. This might be caused by the size effect favorable for Pt/CNTs with a little larger Pt particles since larger-sized Pt particles have been demonstrated to be more active for CO oxidation than smaller ones [42–46]. However, for the potential range lower than −0.3 V, the onset potential for CO oxidation on Pt/GNs (−0.63 V) is evidently lower than that on Pt/CNTs (−0.58 V), and the potential of peak 3 on Pt/GNs is also far lower than on Pt/CNTs. These results indicate that the strength of CO adsorption corresponding to peak 3 shall be far weaker on Pt/GNs than on Pt/CNTs. We tentatively ascribed this difference to the stronger electronic effect on Pt exerted by GNs vs. CNTs. Because the strength of CO adsorption

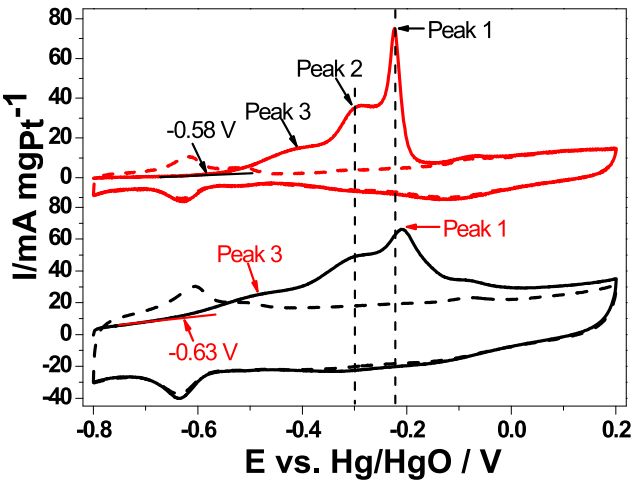


**Fig. 5 – Curves for CO stripping on Pt/CNTs (the upper graph) and Pt/GNs (the lower graph) recorded at 20 mV $s^{-1}$ in 1 M KOH.**

Please cite this article in press as: Wang J, et al., Superior anti-poisoning performance of graphenes versus carbon nanotubes as Pt catalysts supports for formate oxidation, International Journal of Hydrogen Energy (2015), http://dx.doi.org/10.1016/j.ijhydene.2015.11.033

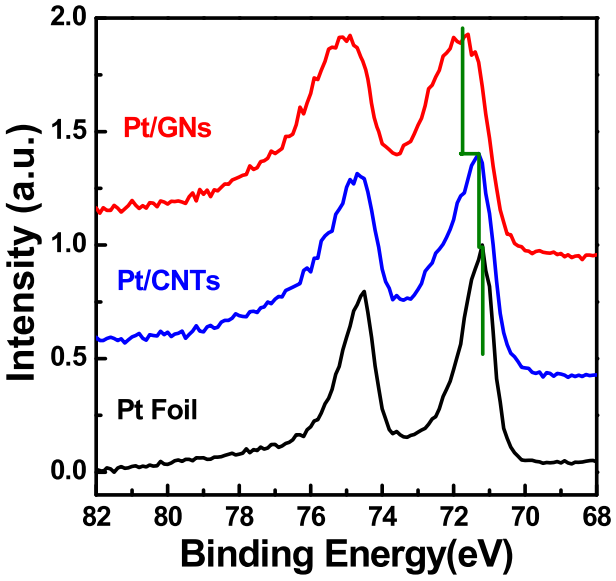


**Fig. 6 – XPS spectra in the Pt 4f region for Pt/CNTs, Pt/GNs and Pt foil.**

corresponding to peak 3 shall be weaker than that which corresponds to peak 1, the size effect on CO oxidation might be negligible, or in other words, indistinguishable for Pt/GNs and Pt/CNTs. In this case, the difference in electronic effects exerted by the two carbonaceous supports, GNs and CNTs, might be discernible, causing a lower onset potential and peak potential for Pt/GNs in comparison with Pt/CNTs.

In fact, the difference in electronic effects exerted by GNs and CNTs can also be reflected from the XPS results. As seen in Fig. 6, there appear two Pt peaks for Pt/CNTs, Pt/GNs or Pt foil that can be ascribed to Pt $4f_{7/2}$ and $4f_{5/2}$ signals, but the binding energy (BE) are slightly different for the three samples. For Pt/CNTs, the BE of Pt $4f_{7/2}$ is about 71.1 eV, which is 0.2 eV higher than that for Pt foil. The slight increase of BE might be due to the final effect [47] for the small size of Pt NPs. While for Pt/GNs, the BE of Pt $4f_{7/2}$ is 0.5 eV higher than that of Pt/CNTs. Because Pt/CNTs and Pt/GNs are not largely different in average Pt size, this further increase of BE can be ascribed to the stronger interaction between Pt particles and GNs. This stronger interaction can then account for the superior anti-poisoning performance of Pt/GNs to Pt/CNTs. That is to say, a stronger binding of Pt particles with GNs produces a greater electron transfer from Pt to GNs, and consequently, the CO species would gain fewer electrons when binding with Pt surface [15,48,49], meaning superior anti-poisoning performance of Pt/GNs in comparison with Pt/CNTs.

Herein we want to emphasize that the main highlight of this study is the electrochemical methods proposed for demonstrating the apparently different anti-poisoning performance of two typical supports (GNs vs. CNTs) for Pt catalysts. However, readers may wonder if there is apparent difference in the catalytic activities of Pt/CNTs and Pt/GNs for formate oxidation. Considering this, we indeed compared the activities based upon the normalized H region area and found that the difference in activities of Pt/CNTs and Pt/GNs is negligible within the error range. Moreover, the peaks of currents for Pt/CNTs and Pt/GNs are also found to be at a nearly same potential. Therefore, it can be concluded that the main advantage of GNs (vs. CNTs) as Pt catalysts supports lies in the superior anti-poisoning effect.

Using the quantitative comparison method proposed in this study, we further calculated the RRR values of three series of reported catalysts (see Table 3) and re-evaluated their anti-poisoning performance in the following contexts. (i) The RRR value of Pt/CNTs-3 is found to be similar to that of Pt/CNTs-1, indicating that the difference of anti-poisoning performance of CNTs-3 and CNTs-1 is negligible. This judgment is in conflict with the original conclusion that CNTs-3 is superior to CNTs-1, the major reason for which is that the authors did not consider the initial difference in CV currents. (ii) Without considering the initial CV currents, the ratio of CA current of Pt/RGO to that of Pd@Pt/RGO is 2.3. However, the RRR value of Pd@Pt/RGO is only 1.4 time that of Pt/RGO, indicating the necessity of considering the initial CV currents. (iii) From the lower RRR of Pt-G-60 than that of Pt-NG-60, we may tentatively assume that the nitrogen doping can improve the anti-poisoning performance of GNs. However, since the time range is only 600 s for case (iii), we want to suggest that longer time range should be needed for CA tests to observe a more distinct difference in anti-poisoning performance.

## Conclusion

A rational method was proposed to quantitatively assess the anti-poisoning performance of DLFCs anode catalysts through evaluating CA currents with reference to CV currents and analyzing the degradation rate of CA currents. Using this method, Pt/CNTs and Pt/GNs were compared as formate oxidation catalysts, and the superior anti-poisoning performance of Pt/GNs was demonstrated. The possible reason is presented from the perspective of the stronger Pt–GNs

**Table 3 – Calculation of the RRR values of three series of reported catalysts.**

| Catalysts | Fuels | CV | | CA | RRR/% |
|---|---|---|---|---|---|
| | | Scan rate | $I_{CV}$ | $I_{CA}$ | |
| Pt@CNT-3 [23] | HCOOH | 30 mV $s^{-1}$ | 146 A $g^{-1}$ | 52 A $g^{-1}$ | 36 |
| Pt@CNT-1 [23] | HCOOH | 30 mV $s^{-1}$ | 82 A $g^{-1}$ | 28 A $g^{-1}$ | 34 |
| Pt/RGO [50] | $CH_3OH$ | 50 mV $s^{-1}$ | 2000 A $g^{-1}$ | 673 A $g^{-1}$ | 34 |
| Pd@Pt/RGO [50] | $CH_3OH$ | 50 mV $s^{-1}$ | 3300 A $g^{-1}$ | 1549 A $g^{-1}$ | 47 |
| Pt-G-60 [51] | $CH_3OH$ | 50 mV $s^{-1}$ | 52 A $g^{-1}$ | 5 A $g^{-1}$ | 10 |
| Pt-NG-60 [51] | $CH_3OH$ | 50 mV $s^{-1}$ | 70 A $g^{-1}$ | 10 A $g^{-1}$ | 14 |

Please cite this article in press as: Wang J, et al., Superior anti-poisoning performance of graphenes versus carbon nanotubes as Pt catalysts supports for formate oxidation, International Journal of Hydrogen Energy (2015), http://dx.doi.org/10.1016/j.ijhydene.2015.11.033

interactions, compared to Pt/CNTs. We hope that this method will prove to be a useful tool for screening and evaluating high quality anode catalysts and various supports in the future.

## Acknowledgments

This research is financially supported by the National Natural Science Foundation of China (U1304215) and the China Scholarship Council (201308410311). This research was also supported by Natural Sciences and Engineering Research Council of Canada (NSERC), Canada Research Chair (CRC) Program, Canada Foundation for Innovation (CFI), and the University of Western Ontario.

## REFERENCES

[1] Ma A, Zhang XF, Li ZS, Wang XY, Ye LT, Lin S. J Electrochem Soc 2014;161:F1224.
[2] Chang JF, Feng LG, Liu CP, Xing W, Hu XL. Angew Chem Int Ed 2014;53:122.
[3] Wang JS, Xi JY, Zhang L, Zhang JJ, Guo X, Zhao JH, et al. Electrochimi Acta 2013;112:480.
[4] Veizaga NS, Rodriguez VI, Rocha TA, Bruno M, Scelza OA, de Miguel SR, et al. J Electrochem Soc 2015;162:F243.
[5] Wang JS, Shi RR, Guo X, Xi JY, Zhao JH, Song CY, et al. Electrochimi Acta 2014;123:309.
[6] Hernandez-Fernandez P, Lund PB, Kallesøe C, Clausen HF, Christensen LH. Int J Hydrogen Energy 2014;40:284.
[7] Sheng WC, Chen S, Vescovo E, Shao-Horn Y. J Electrochem Soc 2012;159:B96.
[8] Lin L, Zhu Q, Xu AW. J Am Chem Soc 2014;136:11027.
[9] Shui JL, Wang M, Du F, Dai LM. Sci Adv 2015;1:e1400129.
[10] Naughton MS, Tornow CE, Bonita Y, Jhong HR, Brushett FR, Gewirth AA, et al. Int J Hydrogen Energy 2013;38:8980.
[11] Jiang RZ, Moton E, McClure JP, Bowers Z. Electrochim Acta 2014;127:146.
[12] Figueiredo MC, Aran-Ais RM, Feliu JM, Kontturi K, Kallio T. J Catal 2014;312:78.
[13] Bandarenka AS, Koper MTM. J Catal 2013;308:11.
[14] Hong JW, Kim D, Lee YW, Kim M, Kang SW, Han SW. Angew Chem Int Ed 2011;50:8876.
[15] Zhu JB, Xiao ML, Zhao X, Li K, Liu CP, Xing W. Chem Commun 2014;50:12201.
[16] Morgan RD, Salehi-khojin A, Masel RI. J Phys Chem C 2011;115:19413.
[17] Zhang YT, Shu HH, Chang G, Ji K, Oyamab M, Liu X, et al. Electrochim Acta 2013;109:570.
[18] Manoharan R, Goodenough JB. J Mater Chem 1992;2:875.
[19] Sun SH, Zhang GX, Gauquelin N, Chen N, Zhou JG, Yang SL, et al. Sci Rep 2013;3:1775.
[20] Kim YT, Matin MA, Kwon YU. Carbon 2014;66:691.
[21] Yoo E, Okata T, Akita T, Kohyama M, Nakamura J, Honma I. Nano Lett 2009;9:2255.
[22] Safavi A, Kazemi H, Kazemi SH. J Power Sources 2014;256:354.
[23] Hsieh CT, Gu JL, Tzou DY, Chu YC, Chen YC. Int J Hydrogen Energy 2013;38:13045.
[24] Huang HJ, Yang SB, Vajtai R, Wang X, Ajayan PM. Adv Mater 2014;26:5160.
[25] Li FH, Guo YQ, Wu T, Liu Y, Wang W, Gao JP. Electrochim Acta 2013;111:614.
[26] Hofstead-Duffy AM, Chen DJ, Sun SG, Tong YYJ. J Mater Chem 2012;22:5205.
[27] Ma L, Chu DR, Chen RR. Int J Hydrogen Energy 2012;37:11185.
[28] Buso-Rogero C, Herrero E, Feliu JM. ChemPhysChem 2014;15:2019.
[29] Hsu CJ, Huang CW, Hao YW, Liu FQ. Int J Hydrogen Energy 2013;38:15532.
[30] Noborikawa J, Lau J, Ta J, Hu SZ, Scudiero L, Derakhshan S, et al. Electrochim Acta 2014;137:654.
[31] Jiang JH, Scott J, Wieckowski A. Electrochim Acta 2013;104:124.
[32] John J, Wang HS, Rus ED, Abruna HD. J Phys Chem C 2012;116:5810.
[33] Jiang JH, Wieckowski A. Electrochem Commun 2012;18:41.
[34] Bartrom AM, Ta J, Nguyen TQ, Her J, Donovan A, Haan JL. J Power Sources 2013;229:234.
[35] Yu XW, Manthiram A. Appl Catal B Environ 2015;165:63.
[36] Zeng L, Tang ZK, Zhao TS. Appl Energy 2014;115:405.
[37] Geng DS, Chen Y, Chen YG, Li YL, Li RY, Sun XL, et al. Energy Environ Sci 2011;4:760.
[38] Wang JS, Xi JY, Bai YX, Shen Y, Sun J, Chen LQ, et al. J Power Sources 2007;164:555.
[39] Wang JS, Guo X, Song CY, Wang LC, Zhao JH, Qiu XP. Acta Phys Chim Sin 2009;25:767.
[40] Li JJ, Wang JS, Guo X, Zhao JH, Song CY, Wang LC. Fuel Cells 2012;12:898.
[41] Zhang ZY, Xin L, Sun K, Li WZ. Int J Hydrogen Energy 2011;36:12686.
[42] Arenz M, Mayrhofer KJJ, Stamenkovic V, Blizanac BB, Tomoyuki T, Ross PN, et al. J Am Chem Soc 2005;127:6819.
[43] Bayati M, Abad JM, Bridges CA, Rosseinsky MJ, Schiffrin DJ. J Electroanal Chem 2008;623:19.
[44] Takasu Y, Iwazaki T, Sugimoto W, Murakami Y. Electrochem Commun 2000;2:671.
[45] Li XX, Qiu XP, Yuan HP, Chen LQ, Zhu WT. J Power Sources 2008;184:353.
[46] Maillard F, Eikerling M, Cherstiouk OV, Schreier S, Savinova E, Stimming U. Faraday Discuss 2004;125:357.
[47] Liu CH, Mao BH, Gao J, Zhang S, Gao X, Liu Z, et al. Carbon 2012;50:3008.
[48] Fampiou I, Ramasubramaniam A. J Phys Chem C 2013;117:19927.
[49] Tang YN, Yang ZX, Dai XQ. J Nanopart Res 2012;14:844.
[50] Kim Y, Noh Y, Lim EJ, Lee S, Choi SM, Kim WB. J Mater Chem A 2014;2:6976.
[51] Xu X, Zhou YK, Yuan T, Li YW. Electrochimi Acta 2013;112:587.

Please cite this article in press as: Wang J, et al., Superior anti-poisoning performance of graphenes versus carbon nanotubes as Pt catalysts supports for formate oxidation, International Journal of Hydrogen Energy (2015), http://dx.doi.org/10.1016/j.ijhydene.2015.11.033